Rare Metal Materials and Engineering
Volume 50, Issue 12, December 2021
Available online at www.rmme.ac.cn

Science Press

Cite this article as: Yan Jikang, Chen Junyu, Qiu Zhesheng. Simulation on ZL201 Aluminum Alloy Sub-frame for Foundry Technology[J]. Rare Metal Materials and Engineering, 2021, 50(12): 4314-4318.

ARTICLE

Simulation on ZL201 Aluminum Alloy Sub-frame for Foundry Technology

Yan Jikang[1], Chen Junyu[1], Qiu Zhesheng[2]

[1] Faculty of Materials Science and Engineering, Kunming University of Science and Technology, Kunming 650093, China; [2] Yunnan Aluminum Co., Ltd, Kunming 650502, China

Abstract: The evolution of microstructures of ZL201 sub-frame during casting was investigated. The processes of casting and cooling solidification were calculated by finite element and thermodynamic theory. The phase compositions were characterized by X-ray diffraction (XRD), and the microstructures were detected by optical microscope (OM) and scanning electron microscopy (SEM). The results show that the simulated results of casting and cooling process are consistent with the experiment. When the pressure is 0.4 MPa, the filling rate of ZL201 sub-frame is 98% and the filling time is 10 s. After heat treatment, the θ phases (Al_2Cu) dissolve into the Al matrix, and form homogeneous solid solution, which increases the grain size.

Key words: ZL201; cellular automation; thermodynamic theory; finite element

Recently, the development of lightweight automobiles has received increasing attention. The rapid growth of car ownership and lightweight automobiles provides an effective measure to mitigate the associated energy and environmental problems[1]. The advantages of the ZL201 aluminum alloy include low density, and excellent corrosion resistance and ductility[2].

The ZL201 aluminum alloy has been widely used in the automobile body, chassis, and powertrain[3]. However, the poor fluidity of ZL201 increases the hot cracking tendency of sub-frame casting[4]. The forming reasons for the poor liquidity are multi-scale and multi-aspect in the foundry technology, such as alloy composition, casting process, and heat treatment[5]. He[6] researched that La and Ce doping can improve the fluidity of ZL205A aluminum alloys, and the length of liquidity is increased by 530 mm compared to the original one. Mousavi[7] analyzed the effect of Sc addition on the solidification behavior of 7108 aluminum alloy castings, and observed that grain size, as well as cracking susceptibility, decrease with increasing the amounts of scandium and that hot cracking is completely eliminated when Sc addition content is above 0.25wt%. In particular, Wei[8] adopted the finite element method to study the mechanisms inducing hot cracking during laser welding of 6xxx aluminum alloys, and accurately predicted the influencing factors of hot cracking in aluminum alloy casting by simulation and calculation, which will significantly reduce the test number and cycle, and increase production efficiency. At present, the randomness of hot cracking makes it impossible to achieve the desired standard solely through experiments. Integrated computing has become a new research in computational solution[9].

In this work, the technological process of a ZL201 sub-frame casting (Fig. 1) was investigated by finite element and thermodynamic theory in the casting and solidification process, and heat treatment. The simulation parameters provide useful reference to optimize the property and microstructure of the sub-frame.

1 Microstructure and Phase Diagrams Simulation

1.1 Meshing models

In order to calculate the microstructure simulation (CAFE) and the temperature field, the surface mesh and volume mesh were divided into nodes and grids with equilateral triangle elements as shown in Fig. 2. The mesh size of the ZL201 sub-frame was 30 mm, and that of samples was 0.3 mm. The cylinder samples were cast with a diameter of 15 mm and a height of 10 mm. The nucleation site was sampled to thoroughly analyze the effects of different alloy compositions

Received date: December 17, 2020
Corresponding author: Yan Jikang, Ph. D., Professor, Faculty of Materials Science and Engineering, Kunming University of Science and Technology, Kunming 650093, P. R. China, E-mail: scyjk@kust.edu.cn

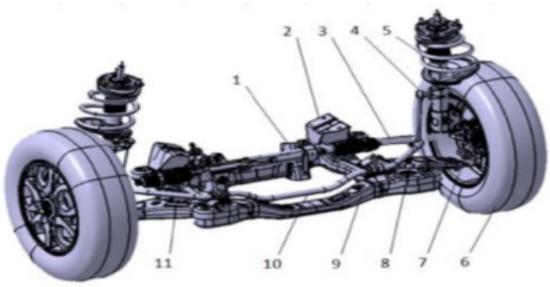

1. steering bracket; 2. mount bracket; 3. steering engine; 4. shock absorber; 5. spring; 6. tire; 7. steering knuckle; 8. stabilizer rod; 9. auxiliary frame; 10. stabilizer bar; 11. control arm

Fig.1 Structure of a sub-frame

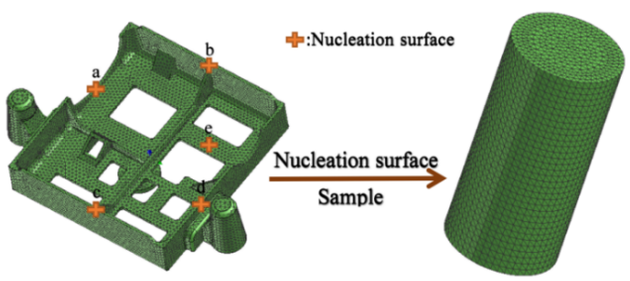

Fig.2 Grids of ZL201 sub-frame casting

on microstructure. The nucleation particle grows in a subdivided mesh. The mesh division should not only ensure the number of nucleated particles in the mesh, but also ensure that the growth of grains cannot exceed the range of a cell.

1.2 Thermophysical parameters

Using Procast software, both casting and heat treatment processes of ZL201 sub-frame were simulated with the composition of alloying elements in Table 1, the mold temperature of 250 °C, the casting temperature of 750 °C and T5. In the ZL201 sub-frame casting model, the solid phase fraction was calculated by the Scheil equation for intracellular grains, as shown in Eq.(1)[10].

$$C_s=k_eC_0(1-f_s)^{k_e-1} \quad (1)$$

Table 1 Chemical composition of the ZL201 auxiliary frame (wt%)

Cu	Mn	Ti	Al
5.0	0.8	0.3	Bal.

where k_e is the effective solute solidification coefficient, C_0 is the initial composition, f_s is the frequency, and C_s is the solute segregation of the solid phase. In the microstructure simulation, the growth coefficient directly determines the growth rate of dendrites. The coefficient of growth can be expressed as Eq.(2) and Eq.(3)[11].

$$\alpha=[\frac{-\rho}{(mc_0)(1-k)^2 2\Gamma k}+\frac{mc_0}{(mc_0)(1-k)^2 D}]\frac{D^2}{\pi^2\Gamma} \quad (2)$$

$$\beta=\frac{D^2}{\pi\Gamma}\cdot\frac{1}{(mc_0)(1-k)^2 D} \quad (3)$$

where m is the liquid phase slope, c_0 is the alloy composition, Γ is the Gibbs-Thompson parameter, D is the liquid diffusion coefficient, k is the equilibrium solute partition coefficient, α is the first level growth coefficient, and β is the second level growth coefficient. The values of the thermophysical parameters and growth coefficients required for the microstructure simulation are listed in Table 2.

The phase diagrams of the ZL201 aluminum alloy were calculated by thermodynamic theory. The simultaneous solution of the above equations was calculated to obtain a series of simultaneous equations. From these equations, the component with the lowest total Gibbs free energy was obtained. According to the results, the cooling and solidification curves and the phase diagrams of the ZL201 aluminum alloy system were drawn by thermodynamic calculation[16].

2 Experiment

The ZL201 sub-frame casting was prepared by the low pressure casting under the pressure of 0.4 MPa, the casting temperature of 750 °C and the casting time of 10 s. The impurity elements include Fe, Si, and B, which are present in concentrations less than 0.01wt%. The metal mold was made from carbon steel C45. The cooling method was air cooling (FilmCo=10, T=25 °C). In T5 heat treatment process, the solution temperature was 548 °C for 8 h, the quenching temperature was about 60 °C, and the aging temperature was 170 °C for 7 h.

Sampling process and sites of sample sections for OM and XRD are shown in Fig. 3. The microstructural sampling process of the ZL201 aluminum alloy is as follows.

(1) As shown in Fig. 2, samples were taken from the aluminum alloy castings. The sampling position of the casting samples was inside the label of (1~3) and they were cut by a

Table 2 Simulation parameters for CAFE fields

Parameter	Numerical value
Coefficient of heat conduction/W·(m^2·K)$^{-1}$ [12]	1050
Heat[13]	FilmCo=10, T=25 °C
Hardening heat gate velocity/cm·s^{-1}	0.24
Coefficient of growth (α, β)	α=4.45×10^{-7}, β=3.74×10^{-6}
Maximum nucleation density (n_{max})/m^3 [14]	1×10^8
Average nucleation and sub-cooling (ΔT_n)/K [14]	0.4
Standard curvature sub-cooling (ΔT_σ)/K [15]	0.1

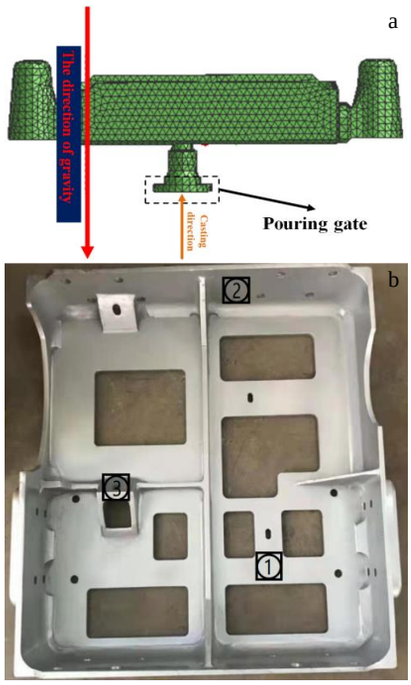

Fig.3 Sketches of sub-frame casting (a) and sampling section (b)

metallographic sample cutter.

(2) The casting samples were ground with 180#, 400#, 800#, and 1200# grit sandpaper.

(3) The ground samples were polished on the polishing machine at a speed of approximately 1000 r/min.

(4) The polished samples were cleaned with anhydrous ethanol (99.99mol%). The sample surface was corroded with hydrofluoric acid (10mol%) for 5~10 s. The observation position of the microstructure is shown in Fig. 4.

3 Results and Discussion

3.1 Filling and solidification process

In the casting process, Fig. 4a shows that the ZL201 sub-frame casting is filled by a low pressure casting technology. The casting time is 10 s, and the filling rate of ZL201 sub-frame is 98%. Fig. 4b shows the process of cooling solidification, and the temperature field is obtained by steady-state analysis during 10~720 min. The initial temperature of the casting is 750 °C. Contacting interface between castings and molds results in a strong heat exchange, which makes the surface temperature of the mold rise from 250 °C to 450 °C. Section A is the first to reach the liquidus temperature at 652 °C. Then, the temperature of the most parts of casting begins to drop. The most of liquid aluminum alloy begins to solidify. When the solidification time is 10 min, the casting center, section B and pouring gate are still liquid, and the temperature of other positions has dropped below the solid phase line, which is induced by the supreme heat dissipation conditions of the casting edge part. The transformation from liquid state to solid state is within 10~60 min, and the phase transition zone begins to spread to the surface of the casting. When solidification time reaches 720 min, the temperature of the

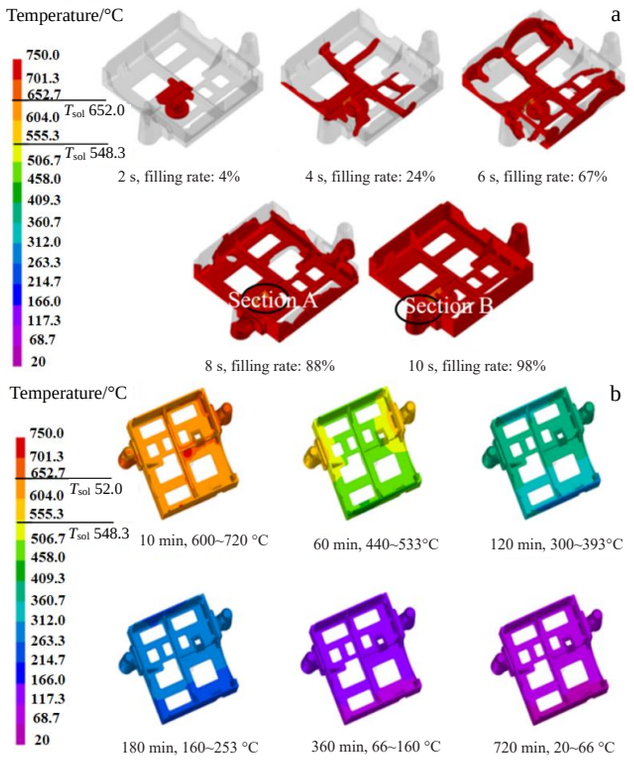

Fig.4 Processes of casting (a) and cooling solidification (b) for ZL201 sub-frame

casting drops to 20~66 °C. Because the internal and external temperature difference is less than 15 °C, the cooling rate of the casting temperature becomes slow. The heat exchange process is basically completed until it is cooled to room temperature.

3.2 Heat treatment

OM microstructures of ZL201 sub-frame and their corresponding CAFE fields before and after heat treatment are shown in Fig.5. Samples are from position 1, 2 and 3 in Fig.3. Fig.6 shows SEM microstructures of ZL201 sub-frame casting befor and after heat treatment. For the unheated samples, the grain size is 16~18 μm. With the heat treatment, the grain size is 20~25 μm. After solution treatment at 548 °C, the atomic diffusion becomes easier, and the θ phase (Al_2Cu) dissolves into the Al matrix in the ZL201, which forms homogeneous solid solution and results in increase of grain size. After the casting is cooled, the composition dissolves into Al matrix to form a supersaturated solid solution, which can improve the ductility and toughness of the sub-frame casting.

XRD patterns of ZL201 sub-frame casting are shown in Fig. 7a. For the unheated treatment samples, the diffraction peaks and 2θ of Al_{fcc} are (111)-38.2°, (200)-45.4°, (220)-65.1°, (311)-77.8° and (222)-82.7°. As shown in Fig. 7b, the phase composition of ZL201 aluminum alloy is calculated by thermodynamic method. ZL201 is mainly composed of Al_{fcc}, Al_3Ti, θ and $Al_{20}Cu_2Mn_3$ phases. The presence of other impurity elements is considered, such as Al_7Cu_2Fe impurity phase. Al-Cu-Mn ternary compound in the ZL201 alloy calcu-

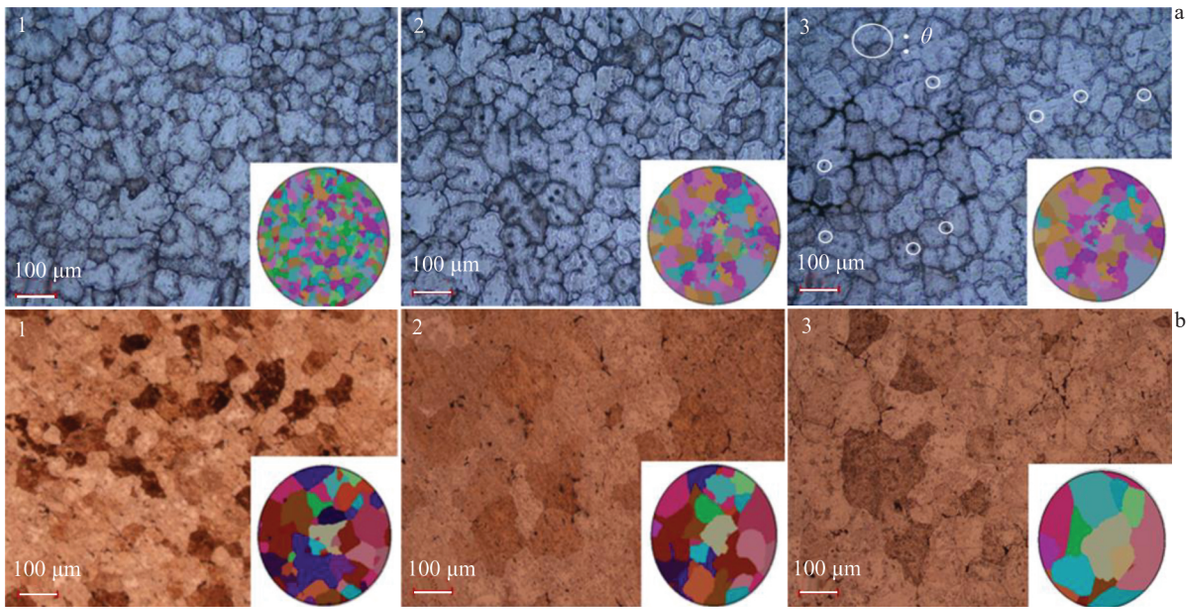

Fig.5 OM corrosion microstructures of ZL201 sub-frame and corresponding CAFE fields (insets) before (a) and after (b) heat treatment sample (1, 2, 3 correspond to positions 1, 2, 3 in Fig.3)

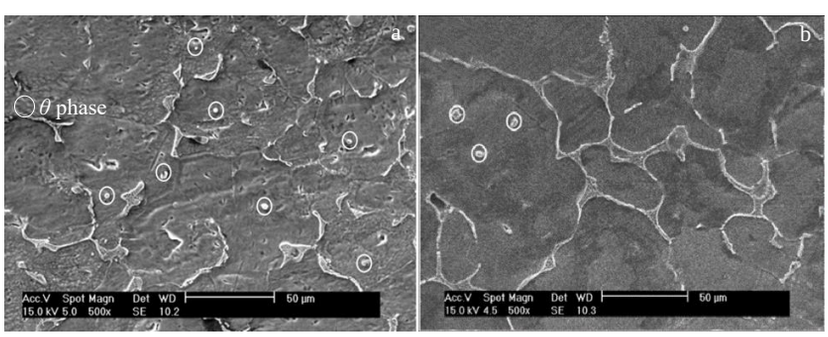

Fig.6 SEM microstructures of ZL201 aluminum alloy sub-frame casting before (a) and after (b) heat treatment

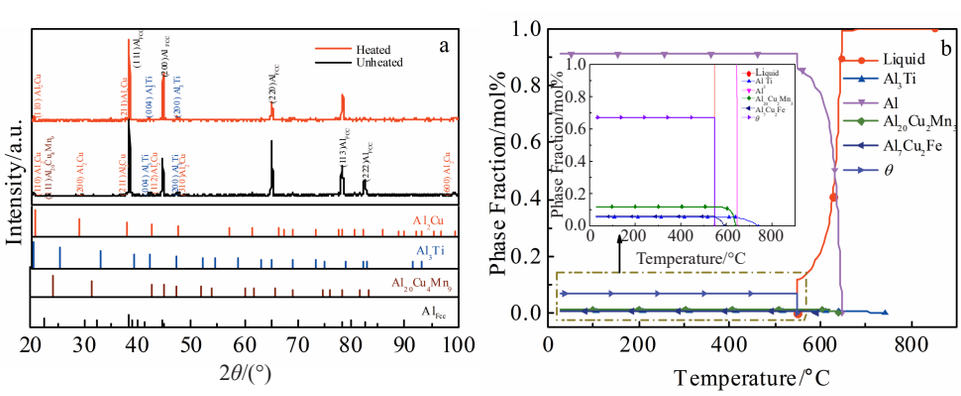

Fig.7 XRD patterns (a) and phase composition (b) obtained by thermodynamic method of ZL201

lated by thermodynamics is $Al_{20}Cu_2Mn_3$, while the detection result of XRD pattern is $Al_{20}Cu_4Mn_9$. According to the comparison between unheated and heated treatment, the Al-Cu-Mn phase disappears after heat treatment, the characteristic peak of the θ phase is reduced, and the characteristic peak strength of Al matrix increases. θ phase (Al_2Cu) dissolves into the Al matrix in the ZL201, which forms homogeneous solid solution. As a result, the grain size increases. After ZL201 sub-

frame is cooled, θ phase dissolves into Al matrix to form a supersaturated solid solution, which can improve the dynamic and toughness of the sub-frame casting.

4 Conclusions

1) The simulated results of casting and cooling process of ZL201 aluminum alloy by finite element and thermodynamic theory are consistent with the experiment. When the pressure is 0.4 MPa, the filling rate of ZL201 sub-frame is 98% and the filling time is 10 s.

2) After heat treatment, the θ phases (Al_2Cu) dissolve into the Al matrix, and form homogeneous solid solution, which results in an increase in the grain size.

References

1 Kim H C, Wallington T J, Sullivan J L *et al*. *Environmental Science & Technology* [J], 2015, 49(16): 10 209

2 Liu D. *Automobile Technology*[J], 1995, 1(7): 12

3 Kang Q, Mao X Y, Lin J *et al*. *Advanced Materials Research*[J], 2013, 816-817: 255

4 Wu Y L, Li C G, Sam F A *et al*. *Metallurgical & Materials Transactions A*[J], 1999, 30(4): 1017

5 Wang P P, Zhao C H, Yi Z Y *et al*. *Journal of Materials Sciences & Technology*[J], 2019, 23(4): 14

6 He Kai, Yan Jikang. *Transactions of Nonferrous Metals Society of China*[J], 2014, 24(11): 3632

7 Mousavi M G, Cross C E, Grong. *Science & Technology of Welding & Joining* [J], 2013, 4(6): 381

8 Wei H, Chen J S, Wang H P *et al*. *Journal of Laser Applications* [J], 2016, 28(2): 22 405

9 Kawalla R, Coung N, Stolnikov A. *Magnesium: Proceedings of the 6th International Conference Magnesium Alloys and Their Applications*[M]. Germany: Wiley - VCH Verlag GmbH & Co. KGaA, 2005

10 Mirihanage W U, Mcfadden S, Browne D J. *Materials Science Forum*[J], 2010, 649: 355

11 Jos E. *Philosophical Magazine*[J], 2011, 91(12): 1705

12 Bozzoli F, Cattani L, Rainieri S *et al*. *Experimental Thermal & Fluid Science*[J], 2013, 59(5): 246

13 Montgomery R B. *Journal of the Atmospheric Sciences*[J], 1947, 4(6): 193

14 Spowart J E, Miracle D B, Mullens H M. *Journal of Non Crystalline Solids*[J], 2004, 336(3): 202

15 Zheng L, Wang Y X, Plawsky J L *et al*. *Langmuir*[J], 2002, 18(13): 5170

16 Wang P. *Journal of Northeastern University, Natural Science*[J], 2009, 45(12): 12

ZL201铝合金副车架铸件的工艺仿真及数值模拟

严继康[1]，陈俊宇[1]，邱哲生[2]

(1. 昆明理工大学 材料科学与工程学院，云南 昆明 650093)

(2. 云南铝业有限公司，云南 昆明 650502)

摘　要：为了探讨铸造过程中ZL201铝合金副车架铸件微观组织的演变历程，基于有限元理论，对ZL201副车架铸件的铸造工艺和微观结构的变化过程进行了分析，采用XRD和OM表征了ZL201铝合金的相组成和金相组织。采用有限元法模拟了ZL201副车架的铸造工艺以及热力学方法计算了ZL201的相组成。结果表明，在C45浇铸模具温度为250 ℃，压力为0.4 MPa，铸造温度为750 ℃的条件下，ZL201副车架铸件填充率为98%，浇铸时间为10 s；经过热处理后，θ相（Al_2Cu）溶解在铝基体中形成固溶体强化相，晶粒尺寸增大。

关键词：ZL201铝合金；元胞自动机；热力学；有限元

作者简介：严继康，男，1972年生，博士，教授，昆明理工大学材料科学与工程学院，云南 昆明 650093，E-mail：scyjk@kust.edu.cn